

Static Dielectric Constants for Liquid Water from 300 K to 350 K at Pressures to 13 MPa Using a New Radio-Frequency Resonator

Gary S. Anderson and Reid C. Miller*

Department of Chemical Engineering, Washington State University, Pullman, Washington 99164

Anthony R. H. Goodwin†

Center for Applied Thermodynamic Studies, University of Idaho, Moscow, Idaho 83844

A stainless steel reentrant cavity with primary resonances at three frequencies has been constructed and used to make dielectric constant measurements on liquid water between 300 K and 350 K, at pressures to 13 MPa. At the frequencies of this study (25 MHz to 250 MHz), there is no evidence of frequency dependence in the water data. Three methods have been used to convert resonant frequencies to dielectric constants. Using a lumped-parameter model recommended recently by NIST investigators, the dielectric constants from the current work agree within 0.1 with the best data available from other recent investigations. Temperature and pressure derivatives of the dielectric constant are nearly identical using all three methods, and they are found to be in reasonable but not perfect agreement with the best available correlation of previous results. A waveguide model approach resulted in dielectric constants about 0.3 higher than accepted values, likely due to uncertainties in geometry and materials properties. A second lumped-parameter approach also failed, likely due to its dependence on measured resonant frequency half widths with water occupying the cavity.

Introduction

The static (zero-frequency) dielectric constant of water has been a quantity of great interest, as it is related to many important physical and biological applications. The dielectric constant and its temperature and pressure derivatives are the fundamental properties that must be known to utilize theories of electrolyte solutions. Example applications include predicting ionic solubilities, important in geochemistry and chemical processing, and analyzing folding in proteins, important in biological processes. Dielectric constants of the highest accuracy are needed to obtain sufficiently accurate values for the temperature and pressure derivatives. Today, the static dielectric constant of water or aqueous solutions cannot be determined with sufficient accuracy from theoretical equations or molecular dynamics, and experimental techniques are still of great interest. Over the past century, many experimental studies have been conducted for water, over a wide range of temperature and pressure; however, some unresolved issues remain, particularly under severe conditions.

All reliable sources of dielectric constant data for water available in the literature (to 1995) have been compiled, evaluated, corrected (where possible), and converted to ITS-90 (Fernandez et al.¹). The data cover temperatures from 238 K to 873 K and pressures from 0.1 MPa to 1189 MPa. There are regions where there are little or no data, particularly at high temperatures and pressures. Also, there are some uncertainties in the pressure and temperature derivatives at common temperatures and pressures. A correlation for the static dielectric constant of water has been developed using this database (Fernandez et al.²).

Historically, capacitance measurements in the audio frequency range have been used to measure the dielectric constant of water. One important disadvantage of this technique is that the water samples must contain very low ionic concentrations to prevent electrode polarization. Some of the static dielectric constant results reported in the literature have been questioned due to contamination. In a recent study (Fernandez et al.³), a concentric-cylinder capacitor was used for capacitance measurements of water at temperatures between 273 and 373 K and at ambient pressure. Water conductivities were maintained within 20% of the lowest possible values, producing data of high accuracy; however, some questions remained at the upper end of this temperature range, where the natural conductivity of water becomes higher.

Measurements using resonant microwave circuits also have been used to obtain dielectric data on substances. These techniques involve an electromagnetic resonator, which has many modes of oscillation when connected to a source of electromagnetic radiation. However, for dielectric measurements, only the fundamental modes of oscillation are needed, at the lowest resonant frequencies. Resonators that oscillate in the radio frequency and microwave ranges have been used for determining the dielectric constant of water and solid insulators, and for other purposes.

NIST investigators (Goodwin et al.⁴) developed a reentrant-type resonator, with a single-lobe extension inside the cavity. It was used to measure dipole moments of polar gases, as well as densities along the phase boundaries for a CO₂ + C₂H₆ mixture near its critical point. The single-lobe extension created one primary inductor and one primary capacitor in the circuit, and therefore one fundamental resonant frequency (near 375 MHz under vacuum). Equations based on waveguide theory, along with conven-

* Corresponding author.

† Current address: Schlumberger-Doll Research, Ridgefield, CT 06877.

tional circuit analysis, were used as a model for calculating the dielectric properties of the fluid occupying the resonator.

The above work was extended (Hamelin et al.⁵) by development of a cavity with two lobes. This cavity was gold-plated and had vacuum resonant frequencies near 216 MHz and 566 MHz. They recommended a lumped-parameter model to analyze the data, using measured vacuum resonant half-widths combined with measured resonant frequencies. This apparatus was used by the same NIST investigators (Hamelin et al.⁶) to measure static dielectric constants of liquid water between 275 K and 400 K at saturation conditions (under the vapor pressure at each temperature). These are likely the most accurate data obtained to date on liquid water at low pressures.

In the present work, an attempt is being made to extend reentrant resonator experimentation to water and aqueous solutions over wide ranges of temperature and pressure. The first resonator designed and tested has three primary resonant frequencies, over a 10-fold range, to ensure that neither polar relaxation nor electrode polarization are causing measured dielectric constants to be frequency dependent.

Experiments

The experimental system reported here is described in greater detail elsewhere (Anderson⁷). A cross-sectional diagram of the radio frequency reentrant cavity is shown in Figure 1. This resonator is constructed from Type-316 stainless steel, which has good corrosion resistance and sufficiently high conductivity to result in small skin depth at the experimental frequencies.

The resonator body is comprised of three main metal parts that connect to form the enclosed cavity. The largest part is a hollow cylinder open at both ends. A lid containing a three-lobed extension forms the bottom end of the cylinder. The outer side of this lid contains two electrical connectors for the microwave cables from the network analyzer, the instrument used to send signals of varying frequency to the cavity. Kovar wires (0.5 mm diameter) are attached to the center conductors of the microwave cables and pass through the lid, becoming half-loop antennae inside the cavity. The loops are offset about 10° from perpendicular to the radial direction, to provide weak coupling with the reentrant cavity circuit. The ends of the wires are inserted into small holes in the lid internal surface. The Kovar wires are sealed into the lid with glass beads that are melted at 613 °C and resolidified around the wires. The portion of the lid exposed to the test fluid had to be resurfaced, because this process of making glass/metal seals reduced the corrosion-resistant properties of the surface layers of the stainless steel.

A cylindrical end plate forms a second closure at the top of the cell. The center of this plate contains the fluid outlet port. The fluid inlet port is located on the side of the cavity near the bottom. Nickel silver O-rings, compressed by use of Allen screws, are used on both ends to maintain pressure seals.

Figure 2 shows the location of the three main capacitors (C1, C2, and C3) and inductors (L1, L2, and L3) and the definitions of all cavity dimensions r_i and z_i . The main capacitors are the small annular gaps between the lobes and the cavity wall, while the main inductors are the toroidal spaces between the lobes. The dimensions of these inductors and capacitors are given in Table 1. The space beyond the third lobe acts as a very weak cylindrical capacitor and has dimensions of $z_4 = 25.916$ mm and $z_5 =$

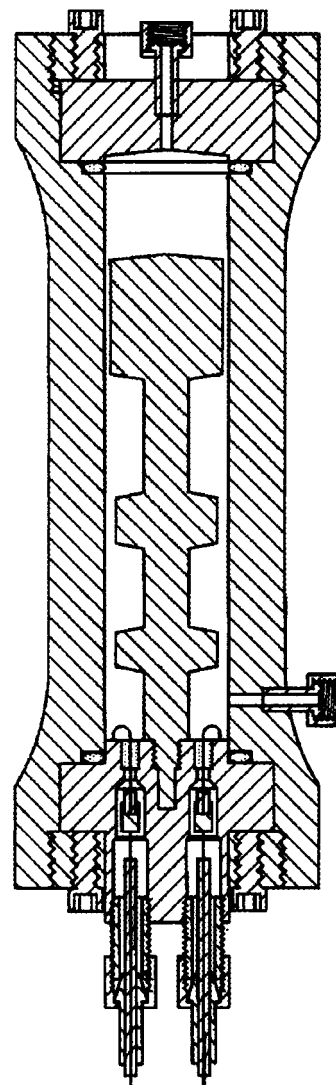


Figure 1. Cross section of the reentrant cavity resonator.

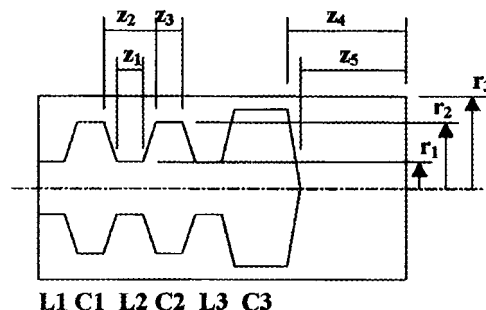


Figure 2. Location of main inductors (L1, L2, and L3) and capacitors (C1, C2, and C3) and definition of all dimensions z_i and r_i .

Table 1. Reentrant Resonator Dimensions for Each Inductor/Capacitor Section As Defined in Figure 2

| section | r_1 /mm | r_2 /mm | z_1 /mm | z_2 /mm | z_3 /mm |
|---------|-----------|-----------|-----------|-----------|-----------|
| L1, C1 | 5.080 | 11.176 | 14.986 | 15.519 | 7.112 |
| L2, C2 | 5.080 | 11.176 | 17.018 | 18.084 | 9.906 |
| L3, C3 | 4.064 | 12.192 | 24.892 | 26.047 | 25.400 |

24.849 mm. The cavity itself has an inner radius of $r_3 = 12.700$ mm. The free volume of the cavity is about 43 cm³.

The resonator was suspended (antennae end down, as shown) in a cylindrical copper vessel containing atmospheric air, which, in turn, was immersed in a stirred water

bath. To minimize temperature gradients, three heavy braided strips of silver-plated copper were used to connect the lid of the copper cylinder to a thick brass ring clamped to the resonator. The copper container was suspended in the water bath by four thin-walled stainless steel tubes. A precision temperature controller was used to maintain the bath temperature constant, with a long-term stability of ± 0.02 K.

Bath temperatures were measured with calibrated platinum resistance thermometers. Reported temperatures are believed accurate to ± 0.03 K. A 20 MPa double-revolution bourdon tube gauge was used throughout the experiments. The gauge was calibrated against a liquid-lubricated piston gauge, and the pressures reported are believed accurate to ± 0.01 MPa.

A network analyzer, operable from 300 kHz to 6 GHz, was used to excite the resonator at a series of fixed frequencies. The signal from the network analyzer was sent to the cavity through one of the two coaxial feedthroughs. The return signal that describes the transmission characteristics of the resonator was returned through the second feedthrough. Network analyzer results were automatically downloaded to a laboratory computer for analysis. The three resonance frequency peaks were fit to the following theoretical resonance function:

$$S_{21}(f_s) = \frac{Af_s}{f_s^2 - F^2} + B + Cf_s \quad (1)$$

The term f_s represents the frequency of the signal sent from the network analyzer to the cavity. Equation 1 was fit by least squares to the network analyzer complex S_{21} scattering parameter data, with the complex constants F , A , B , and C as fitting parameters. The C term was always checked for statistical significance and omitted when appropriate. The resonant frequency is the complex constant $F = f + ig$. Thus, f is the real component of the resonant frequency of the cavity, and g is the resonance half-width, which is an indicator of dissipative processes within the resonator.

Frequency data (201 points) were taken repeatedly in the vicinity of each of the three peaks (range = $f \pm 2g$) and averaged to eliminate most of the effects of noise. Both f and g , and their standard deviations, were determined to the nearest 100 Hz. For vacuum, helium, and argon measurements, the fractional uncertainty (the ratio of the standard deviation in frequency to the frequency itself) was typically $< 3.0 \times 10^{-6}$. For frequency measurements with water as the test fluid, the fractional uncertainty was always $< 1.0 \times 10^{-5}$ for the low-frequency mode and $< 4.0 \times 10^{-6}$ for the middle- and high-frequency modes.

The resonant frequencies of the cavity were determined under vacuum prior to each filling of the cell. For both helium and argon, data were taken on five isotherms between 298 and 340 K. For each isotherm studied, frequency measurements were taken at 1.5 MPa increments between 0 and 13 MPa, starting at the high-pressure end and working down. After frequency measurements at the lowest pressure (0.1 MPa), the cell was evacuated and another vacuum frequency measurement was made. The set point temperature for the isothermal bath was then increased approximately 10 K, and the system was again left to equilibrate under vacuum.

Diagrams of the experimental setup for the experiments with gases and with water can be found elsewhere.⁷ Gases were fed to the cell directly from high-pressure cylinders. For water measurements, samples of double-deionized

water were stored in a Nalgene container. A hand-operated, high-pressure pump was used to draw a portion of the water sample from the container, from which the sample was fed through the inlet port near the bottom of the resonator cavity. The water exited the resonator through the fluid outlet line at the top of the cavity, which opened into an expansion volume. Water was fed until the expansion volume was approximately half full. The space above the liquid in the expansion volume was then repeatedly pressurized with nitrogen and briefly evacuated to remove any bubbles from the cell.

The helium gas used in the dilation calibrations was 99.995 mol % minimum purity, with a total hydrocarbon content < 0.5 ppm. The argon gas used in the test experiments was 99.999 mol % minimum purity. Conductivities of the water samples were measured using a conductance meter calibrated with a standard 0.0200 M KCl solution. The conductivity of the purest water known is about $5.5 \mu\text{S}\cdot\text{m}^{-1}$ at 298.15 K. Distilled water in equilibrium with air has a conductivity of $\sim 70 \mu\text{S}\cdot\text{m}^{-1}$ at this temperature. In the present work, double-deionized water in equilibrium with air was used, with an initial conductivity $< 130 \mu\text{S}\cdot\text{m}^{-1}$, the lower limit of sensitivity for the measurement system. Samples after removal from the cell generally ranged from 200 to $400 \mu\text{S}\cdot\text{m}^{-1}$, probably due to leaching of ions from the equipment during experiments. Such values do not have significant impact on dielectric constants calculated from the models. In fact, conductivities $> 1000 \mu\text{S}\cdot\text{m}^{-1}$ are required to increase the dielectric constants from the waveguide model by 0.02% at the frequencies of this study.⁷

Data Analysis

Both distributed- and lumped-parameter models of the current microwave resonator have been used to convert resonant frequency data into dielectric constants. The most satisfactory method was found to be a lumped-parameter model recommended by recent investigators at NIST (Hamelin et al.^{5,6}). The only difference in the current analysis is that no external coupling corrections are needed, due to the very weak coupling employed in the current resonator.

A resonant condition in terms of capacitive and inductive sections for any fundamental mode can be written, solved for dielectric constant, and simplified by incorporating the vacuum resonant condition. Incorporating quality factors ($Q = f/2g$), to first order in Q^{-1} , the working equation for dielectric constant becomes

$$\epsilon = \left(\frac{F_0}{F}\right)^2 \frac{1 + (-1 + j)(1/Q)}{1 + (-1 + j)(1/Q_0)} \quad (2)$$

This working equation can be applied to the f , g , f_0 , and g_0 measurements to directly determine dielectric constants, as long as external coupling is sufficiently weak, fluid electrical conductivity is small, and Q is sufficiently large so that terms in $(1/Q)^2$ are negligible. A modification of eq 2, suggested by the NIST investigators, involves replacing Q^{-1} in the correction term with $(ff_0)^{1.5}Q_0^{-1}\epsilon$, which follows directly from standard relations between resistance, skin depth, and frequency

$$\epsilon = \left(\frac{F_0}{F}\right)^2 \frac{1 + (-1 + j)(ff_0)^{1.5}(1/Q_0)\epsilon}{1 + (-1 + j)(1/Q_0)} \quad (3)$$

This approach has the advantage of reducing the dependence of results on measurements of resonant half-width

Table 2. Constants for Eq 4 Determined by Least-Squares Fits of Vacuum and Helium Resonant Frequencies

| mode | f_0/MHz | $10^5\alpha/^\circ\text{C}^{-1}$ | $10^5\beta/\text{MPa}^{-1}$ | g_0/MHz |
|------|------------------|----------------------------------|-----------------------------|------------------|
| low | 219.0723 | 1.620 | 18.7 | 0.948 |
| mid | 1039.8677 | 1.724 | 4.07 | 3.112 |
| high | 2066.0665 | 1.600 | 3.09 | 4.142 |

with water in the cell, where the quality factors are significantly smaller than those under vacuum conditions. Equation 3 was used to analyze the water results in the recent NIST study (Hamelin et al.⁶). This equation was taken as the basis for reported dielectric constants in the current work. As discussed below, dielectric constants for liquid water have been calculated from eq 2 and compared with the eq 3 results.

To apply these lumped-parameter models, the vacuum and helium resonance data were analyzed to obtain f_0 and g_0 as functions of temperature (t) and pressure (P):

$$f_0 = f_{00}(1 - \alpha t)(1 + \beta P)$$

$$g_0 = g_{00} \quad (4)$$

The constants f_{00} , α , and β were determined by least-squares fit, using measured vacuum frequencies, along with helium resonant frequency data taken at five temperatures between 298 K and 340 K, at pressures to 10 MPa (Anderson⁷). The virial form of the Clausius–Mossotti function was truncated after two terms to calculate helium dielectric constants. The first dielectric virial coefficient, A_e , was taken as $0.517\,248\text{ cm}^3\cdot\text{mol}^{-1}$ (Weinhold⁸), and the second dielectric virial coefficient as $0.13\text{ cm}^6\cdot\text{mol}^{-2}$ (White and Guggen⁹). The helium molar densities were obtained from an equation of state developed by Lemmon et al.,¹⁰ which gives helium densities to $\pm 0.1\%$.

The parameters for eq 4, determined from least-squares fits of the vacuum and helium data, are given in Table 2. Although measured g_0 values are a very weak function of temperature and pressure, treating this parameter as a constant for each mode does not significantly effect calculated dielectric constants. No adjustments were necessary when this calibration was applied to the liquid water data.

Distributed-parameter models, based on waveguide theory, were also employed. As a first approximation, the RF resonator was modeled as having impedances arising only from the three main capacitors and three main inductors. Using standard equations for concentric cylinders, and conventional circuit analysis, a single equation may be derived that describes the resonance conditions of the cavity:

$$\omega^2[L_1C_1 + (L_1 + L_2)C_2 + (L_1 + L_2 + L_3)C_3] - \omega^4[L_1C_1(L_2C_2 + L_2C_3 + L_3C_3) + (L_1 + L_2)L_3C_2C_3] + \omega^6[L_1L_2L_3C_1C_2C_3] = 1 \quad (5)$$

The inductance and capacitance of each section can be calculated from resonator dimensions using standard formulas (Goodwin et al.⁴). The angular frequency ω under vacuum conditions can be determined iteratively from eq 5. This simple model predicts three primary vacuum resonant frequencies that are significantly higher (by 13% to 27%) than those experimentally observed. Additional impedances are present in the resonator, which have not been taken into account in this simple model.

Use of waveguide theory to include resistance effects, fringe and end capacitances, induction effects for the

capacitors, and capacitive effects for the inductors improves the model significantly. The waveguide model was exactly as given previously (Goodwin et al.⁴), except that fluid conductance terms were retained, resulting in slightly modified series and parallel T-equivalent impedances for each inductive and capacitive section of the resonator. This analysis results in an equivalent circuit with 31 separate impedances, which have been incorporated into a series of nested circuit analysis equations.⁷ The only unknowns in this system of equations are the resonant frequencies and the fluid dielectric constant (which appears in each capacitance term). If the resonant frequencies are known experimentally, the dielectric constant can be determined in an iterative fashion for each frequency.

With this waveguide model, small but significant deviations (2, 6, and 7% from low to high modes) are still found between predicted and measured vacuum resonant frequencies, with the predictions larger than the measured values. This may be due in part to imprecise dimensions, including the effect of imperfect centering of the central mandrel in the outer shell. Finite element solutions to Maxwell's equations for the three-lobed cell geometry, assuming infinite conductivity walls, result in predicted vacuum resonant frequencies higher than the measured values by 8, 6, and 1%, again for low to high modes.

To force the waveguide model to reproduce the experimental vacuum resonant frequencies, and to incorporate dilation effects by helium calibration, the analytical equations used for the capacitances of the three main capacitors were replaced by empirical functions of temperature and pressure.⁷ It should be noted that the maximum dilation correction for temperature would impact the dielectric constant by 0.2%, while the maximum correction for pressure would amount to 0.5%. Thus, it is unlikely that small uncertainties in these corrections are significant. Corrections for dilation were not made to the fringe capacitances, to the end capacitance, or to the capacitance elements in the inductive sections, because these capacitances are small compared with the main capacitances, and the related dilation corrections would be very small.

Argon as a Test Fluid

The usefulness of the multilobe resonator for accurately determining the dielectric properties of fluids was first examined by tests with argon. Experimental resonant frequency data for argon were taken on five isotherms between 300 K and 340 K, at pressures to 10.5 MPa. The dielectric constant corresponding to each resonant frequency was calculated using the waveguide model with calibration, as described above. First, dielectric virial coefficients for argon were calculated from the dielectric constants using the Clausius–Mossotti equation. A second dielectric virial coefficient was taken from the literature ($1.22\text{ cm}^6\cdot\text{mol}^{-2}$ at 303.15 K, from Bose and Cole¹¹). The small temperature dependence of the dielectric virial coefficient was neglected. Molar densities were calculated using the same form of equation of state as that for helium.¹⁰

Using the argon data for all modes, for all temperatures, and for pressures > 3 MPa, the average value for the first dielectric virial coefficient from the current work is $(4.137 \pm 0.009)\text{ cm}^3\cdot\text{mol}^{-1}$. At pressures < 3 MPa, the dielectric constants are very close to unity, and the scatter in the calculated first dielectric virial coefficient becomes large. The value quoted here is the same value reported in another recent investigation (Goodwin et al.⁴), but with a somewhat larger uncertainty. The current value is about

Table 3. Experimental Dielectric Constants and Derived Temperature and Pressure Derivatives for Liquid Water

| $T/^\circ\text{C}$ | P/MPa | ϵ | $(\partial\epsilon/\partial T)/\text{K}^{-1}$ | $(\partial\epsilon/\partial P)/\text{MPa}^{-1}$ |
|--------------------|----------------|------------|---|---|
| 28.50 | 0.100 | 77.166 | -0.349 | 0.0362 |
| | 1.000 | 77.200 | -0.349 | 0.0362 |
| | 4.060 | 77.309 | -0.350 | 0.0362 |
| | 6.959 | 77.414 | -0.350 | 0.0362 |
| | 9.909 | 77.521 | -0.351 | 0.0362 |
| | 12.160 | 77.604 | -0.351 | 0.0362 |
| 34.99 | 0.100 | 74.916 | -0.340 | 0.0353 |
| | 1.000 | 74.948 | -0.340 | 0.0353 |
| | 3.995 | 75.053 | -0.340 | 0.0353 |
| | 7.025 | 75.160 | -0.341 | 0.0353 |
| | 10.009 | 75.265 | -0.341 | 0.0353 |
| | 12.572 | 75.356 | -0.342 | 0.0353 |
| 44.95 | 0.100 | 71.622 | -0.325 | 0.0338 |
| | 1.005 | 71.652 | -0.325 | 0.0338 |
| | 4.030 | 71.753 | -0.325 | 0.0338 |
| | 6.995 | 71.854 | -0.326 | 0.0338 |
| | 10.010 | 71.955 | -0.326 | 0.0338 |
| | 12.350 | 72.036 | -0.327 | 0.0338 |
| 55.37 | 0.100 | 68.303 | -0.309 | 0.0337 |
| | 1.007 | 68.336 | -0.309 | 0.0337 |
| | 4.012 | 68.437 | -0.310 | 0.0337 |
| | 7.018 | 68.538 | -0.310 | 0.0337 |
| | 9.975 | 68.637 | -0.311 | 0.0337 |
| | 12.665 | 68.727 | -0.311 | 0.0337 |
| 64.62 | 0.098 | 65.510 | -0.295 | 0.0335 |
| | 1.005 | 65.541 | -0.295 | 0.0335 |
| | 4.012 | 65.640 | -0.296 | 0.0335 |
| | 6.999 | 65.739 | -0.296 | 0.0335 |
| | 9.965 | 65.839 | -0.297 | 0.0335 |
| | 11.765 | 65.902 | -0.297 | 0.0335 |
| 75.15 | 0.100 | 62.475 | -0.279 | 0.0327 |
| | 1.010 | 62.506 | -0.280 | 0.0327 |
| | 4.061 | 62.606 | -0.280 | 0.0327 |
| | 7.020 | 62.701 | -0.280 | 0.0327 |
| | 9.945 | 62.798 | -0.281 | 0.0327 |
| | 11.263 | 62.841 | -0.281 | 0.0327 |

0.07% below the very precise result of (4.1397 ± 0.0006) $\text{cm}^3\cdot\text{mol}^{-1}$ reported much earlier.¹¹ The multilobe reentrant resonator and the waveguide electrical model of the cavity are therefore suitable for dielectric measurements on nonpolar gases such as argon. However, argon results do not indicate with what accuracy the resonator and accompanying model can be used to measure the dielectric properties of a dense polar liquid such as water.

Results for Water

For liquid water, experiments were performed on six isotherms between 300 K and 350 K, with pressures to 13 MPa. Dielectric constants have been calculated using the waveguide model and the two lumped-parameter models. The results for the waveguide model have been reanalyzed, but they are only slightly different from those reported previously.⁷ Comparisons of dielectric constants have been made using values averaged over the three resonant modes. For the waveguide model and the eq 3 lumped-parameter model, deviations from the three-mode average are small (<0.1%), and the pattern for dielectric constant versus frequency is nearly uniform for all experimental conditions. The middle mode yields the high value for the waveguide model and the low value for the eq 3 lumped-parameter model. For the eq 2 lumped-parameter model, deviations from the three-mode average are much larger, and the pattern of deviations is less uniform. In no case is there evidence of systematic frequency dependence in the data.

Dielectric constants calculated from the eq 3 lumped-parameter model are presented for all experimental conditions in Table 3. These dielectric constants are averaged values for the three resonant frequencies of the cavity.

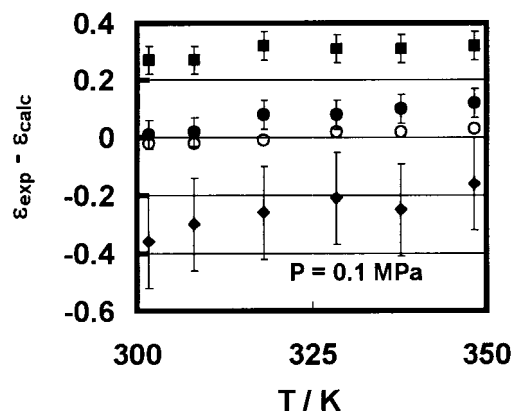


Figure 3. Deviations in liquid water dielectric constant from the correlation of Fernandez et al.:² ●, current results using eq 3; ○, Hamelin et al.;⁶ ■, current results using a waveguide model; ◆, current results using eq 2.

In Figure 3, deviations between experimental dielectric constants (from all three models) and those calculated from the recent published correlation² are plotted versus temperature at 0.1 MPa. The error bars on the experimental data represent the magnitude of the differences between the three modes (discussed in the previous paragraph), plus estimated small combined errors due to uncertainties in temperature, pressure, and ionic impurity level. It is believed that these error bars then represent the precision of the current measurements. Also shown on the figure are points from the equation reported by NIST investigators⁶ as closely fitting their extensive data set at saturation pressures.

The current results from the eq 3 lumped-parameter model are in agreement with the correlation, and with the recent NIST data,⁶ within about 0.1 in dielectric constant. The waveguide model yields dielectric constants about 0.3 above accepted values. These systematic errors are likely due to uncertainties in geometry and in the properties of the stainless steel. The other lumped-parameter model (eq 2) yields dielectric constants about 0.3 below accepted values, with much increased scatter between modes (larger error bars). In this case, the problem is likely due to inaccuracies in measured half-widths when the cell contains liquid water. This shows up as inaccuracies in the quality factors Q , which form the basis for the correction term in eq 2. By appropriate modification of the reentrant cavity, these model results could be brought into better internal agreement. This could be accomplished by use of a one-lobed cell or a two-lobed cell with closer spaced resonant frequencies (simpler geometry) and by obtaining much larger Q factors (e.g., by using a different material of construction or by gold plating the inside of the reentrant cavity).

The dielectric constants reported in Table 3 (determined from the lumped-parameter approach of eq 3) have been fit by least squares to an empirical equation, with the result

$$\epsilon = 78.382[1 - (4.5230 \times 10^{-3})(\theta^\circ\text{C} - 25) + (9.5592 \times 10^{-6})(\theta^\circ\text{C} - 25)^2] \times [1 + (4.8618 \times 10^{-4})(P/\text{MPa})] \quad (6)$$

The standard deviation for the fit is 0.009 in the dielectric constant. The first temperature derivatives from all models are in excellent agreement with each other, and they are well represented by analytical derivatives of eq 6. The first pressure derivatives from eq 6 seem to diverge somewhat

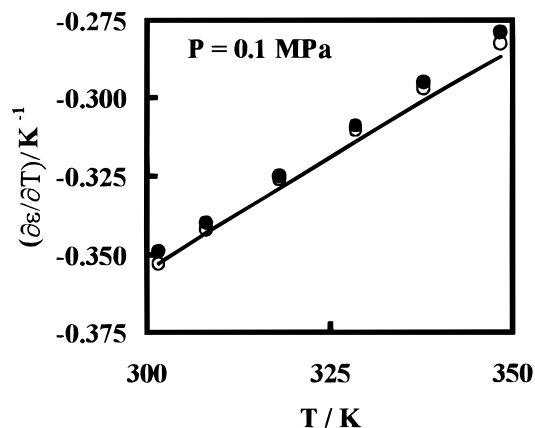


Figure 4. First temperature derivative of the dielectric constant for liquid water: —, from the correlation of Fernandez et al.;² ●, current results; ○, calculated from the data fit of Hamelin et al.⁶

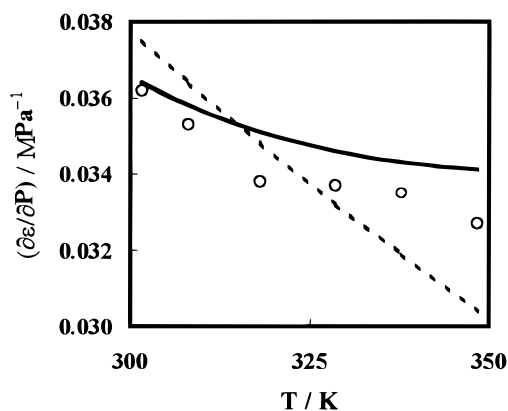


Figure 5. First pressure derivative of the dielectric constant for liquid water: —, from the correlation Fernandez et al.;² ○, current results from fits of individual isotherms; · · ·, current results from derivatives of eq 6.

from values determined from fits of individual isotherms, especially at the highest temperatures studied, as shown below.

First temperature derivatives ($\partial\epsilon/\partial T$) were determined from eq 6 and are listed in Table 3. In Figure 4, they are compared (as a function of temperature at 0.1 MPa) with values from the correlation² and with the recent NIST results.⁶ The values from the present work are less negative than the correlation, with an average deviation of 1%, which is the estimated uncertainty level for the correlation. The NIST results are intermediate, being in better agreement with the correlation at the lower temperatures. The average second temperature derivative between 300 K and 350 K from the current work is in good agreement with the correlation, as can be seen from Figure 4.

First pressure derivatives ($\partial\epsilon/\partial P$) were calculated from linear fits of individual isotherms, and the results are presented in Table 3. Thus, no pressure dependence for this derivative function could be determined from the current work. In Figure 5, first pressure derivatives versus temperature (from Table 3) are compared with values from derivatives of eq 6 and with correlation predictions² at 10.0 MPa. The average deviation from the correlation is about 3%, which is near the estimate of accuracy for the correla-

tion. The current data indicate a slightly larger drop-off with temperature for this derivative function.

The pressure derivatives from the correlation are in excellent agreement with those from a careful study some years ago by Dunn and Stokes.¹² In this work, a concentric cylinder capacitor was used, but data were taken as a function of frequency and extrapolated to high frequency to eliminate electrode polarization effects. Dilation effects were eliminated by pressure equalization methods. Measurements to 100 MPa were made, allowing quite accurate pressure derivatives to be determined. It is interesting to note that the current temperature derivatives are in near perfect agreement with this earlier investigation, while current pressure derivatives show an average deviation of ~2%, consistent with the lower accuracy for this quantity in the current work. Thus, two greatly different methods have been shown to yield temperature and pressure derivatives in good agreement, which lends additional credence to the accuracy of both studies.

Acknowledgment

The authors wish to thank the Gas Research Institute for use of some co-located equipment during this investigation.

Literature Cited

- (1) Fernandez, D. P.; Mulev, Y.; Goodwin, A. R. H.; Levelt Sengers, J. M. H. A Database for the Static Dielectric Constant of Water and Steam. *J. Phys. Chem. Ref. Data* **1995**, *24*, 33–69.
- (2) Fernandez, D. P.; Goodwin, A. R. H.; Lemmon, E. W.; Levelt Sengers, J. M. H.; Williams, R. C. A Formulation for the Static Permittivity of Water and Steam at Temperatures from 238 K to 873 K at Pressures up to 1200 MPa, including Derivatives and Debye–Hückel Coefficients. *J. Phys. Chem. Ref. Data* **1997**, *26*, 1125–1166.
- (3) Fernandez, D. P.; Goodwin, A. R. H.; Levelt Sengers, J. M. H. Measurements of the Relative Permittivity of Liquid Water at Frequencies in the Range of 0.1 to 10 kHz and at Temperatures Between 273.1 and 373.2 K at Ambient Pressure. *Int. J. Thermophys.* **1995**, *16*, 929–955.
- (4) Goodwin, A. R. H.; Mehl, J. B.; Moldover, M. R. Reentrant Radio-Frequency Resonator for Automated Phase-Equilibria and Dielectric Measurements in Fluids. *Rev. Sci. Instrum.* **1996**, *67*, 4294–4303.
- (5) Hamelin, J.; Mehl, J. B.; Moldover, M. R. Resonators for Accurate Dielectric Measurements in Conducting Liquids. *Rev. Sci. Instrum.* **1998**, *69*, 255–260.
- (6) Hamelin, J. O.; Mehl, J. B.; Moldover, M. R. The Static Dielectric Constant of Liquid Water Between 274 and 418 K Near the Saturated Vapor Pressure. *Int. J. Thermophys.* **1998**, *19*, 1359–70.
- (7) Anderson, G. S. A Radio-Frequency Resonator for Dielectric Measurements of Water and Industrially-Important Aqueous Solutions. M.S. Thesis, Washington State University, 1997.
- (8) Weinhold, F. Mass Polarization and Breit-Pauli Corrections for the Polarizability of ⁴He. *J. Phys. Chem.* **1982**, *86*, 1111–1116.
- (9) White, M. P.; Guban, D. Direct Measurements of the Dielectric Virial Coefficients of ⁴He between 3 K and 18 K. *Metrologia* **1992**, *29*, 37–57.
- (10) Lemmon, E. W.; Jacobsen, R. T.; Penoncello, S. G.; Beyerlein, S. W. *Computer Programs for Calculating Thermodynamic Properties of Fluids of Engineering Interest*, Report 95-1; Center for Applied Thermodynamic Studies, University of Idaho: 1995.
- (11) Bose, T. K.; Cole, R. H. Dielectric and Pressure Virial Coefficients of Imperfect Gases. II. CO₂–Argon Mixtures. *J. Chem. Phys.* **1970**, *52*, 140–147.
- (12) Dunn, L. A.; Stokes, R. H. Pressure and Temperature Dependence of the Electrical Permittivities of Formamide and Water. *Trans. Faraday Soc.* **1969**, *65*, 2906–2912.

Received for review December 8, 1999. Accepted March 8, 2000.

JE9903092